Nonlocal Description of the Nuclear Interaction

L. C. Chamon[1], B. V. Carlson[2], L. R. Gasques[1], D. Pereira[1], C. De Conti[2], M. A. G. Alvarez[1], M. S. Hussein[1], M. A. Cândido Ribeiro[3], E. S. Rossi Jr.[1], and C. P. Silva[1]

1. Departamento de Física Nuclear, Instituto de Física da Universidade de São Paulo, Caixa Postal 66318, 05315-970, São Paulo, SP, Brazil

2. Departamento de Física, Instituto Tecnológico de Aeronáutica, Centro Técnico Aeroespacial, São José dos Campos, SP, Brazil

3. Departamento de Física, Instituto de Biociências, Letras e Ciências Exatas, Universidade Estadual Paulista, São José do Rio Preto, SP, Brazil

Received on 30 October, 2002

Extensive systematizations of theoretical and experimental nuclear densities and of optical potential strengths extracted from heavy-ion elastic scattering data analyses at low and intermediate energies are presented. The energy-dependence of the nuclear potential is accounted for within a model based on the nonlocal nature of the interaction. The systematics indicates that the heavy-ion nuclear potential can be described in a simple global way through a double-folding shape, which basically depends only on the density of nucleons of the partners in the collision. The possibility of extracting information about the nucleon-nucleon interaction from the heavy-ion potential is investigated.

I Introduction

The optical potential plays a central role in the description of heavy-ion collisions, since it is widely used in studies of the elastic scattering process as well as in more complicated reactions through the DWBA or coupled-channel formalisms. This complex and energy-dependent potential is composed of the bare and polarization potentials, the latter containing the contribution arising from nonelastic couplings. In principle, the bare (or nuclear) potential between two heavy ions can be associated with the fundamental nucleon-nucleon interaction folded into a product of the densities of the nuclei [1]. Apart from some structure effects, the shape of the nuclear density along the table of stable nuclides is nearly a Fermi distribution, with diffuseness approximately constant and radius given roughly by $R = r_0\ A^{1/3}$, where A is the number of nucleons of the nucleus. Therefore, one could expect a simple dependence of the heavy-ion nuclear potential on the number of nucleons of the partners in the collision.

The elastic scattering is the simplest process that occurs in a heavy-ion collision because it involves very little rearrangement of matter and energy. Therefore, this process has been studied in a large number of experimental investigations, and a huge body of elastic cross section data is currently available. The angular distribution for elastic scattering provides unambiguous determination of the real part of the optical potential only in a region around a particular distance [2] hereafter referred as the sensitivity radius (R_S). At energies close to the Coulomb barrier the sensitivity radius is situated in the surface region. In this energy region, the systematization [3, 4] of experimental results for potential strengths at the sensitivity radii has provided an universal exponential shape for the heavy-ion nuclear potential at the surface region.

In a recent review article [2] the phenomenon of rainbow scattering was discussed, and it was emphasized that the real part of the optical potential can be unambiguously extracted also at very short distances from heavy-ion elastic scattering data at intermediate energies. However, differently from the case for the surface region (low energy), a systematization of potential strengths at the inner distances has not been performed up to now, probably because the resulting phenomenological interactions have presented significant dependence on the bombarding energies. Several theoretical models have been developed to account for this energy-dependence through realistic mean field potentials. A recent model [5, 6, 7, 8] associates the energy-dependence of the heavy-ion bare potential with nonlocal quantum effects related to the exchange of nucleons between target and projectile. Using this model, we have realized [8] a systematization of potential strengths extracted from elastic scattering data analyses, considering both: low (near-barrier) and intermediate energies. The systematics confirms that the heavy-ion nuclear potential can be described in a very simple global way.

II The nuclear densities

According to the double-folding model, the heavy-ion nuclear potential depends on the nuclear densities of the nuclei in collision. Thus, a systematization of the potential

requires a previous systematization of the nuclear densities. We adopt the two-parameter Fermi (2pF) distribution (Eq. 1) to describe the nuclear densities.

$$\rho(r) = \frac{\rho_0}{1 + exp\left(\frac{r-R_0}{a}\right)} \quad (1)$$

In our theoretical calculations, the charge distribution of the nucleus (ρ_{ch}) has been obtained by folding the proton distribution of the nucleus (ρ_p) with the intrinsic charge distribution of the proton in free space (ρ_{chp})

$$\rho_{ch}(r) = \int \rho_p(\vec{r'})\ \rho_{chp}(\vec{r} - \vec{r'})\ d\vec{r'}\ , \quad (2)$$

where ρ_{chp} is an exponential with diffuseness $a_{chp} = 0.235\ fm$. In an analogous way, we have defined the matter density of the nucleus by folding the nucleon distribution of the nucleus with the intrinsic matter distribution of the nucleon, which is assumed to have the same shape of the intrinsic charge distribution of the proton. For convenience, the charge and matter distributions are normalized to the number of protons and nucleons, respectively.

In order to systematize the heavy-ion nuclear densities [8], we have calculated theoretical distributions for a large number of nuclei using the Dirac-Hartree-Bogoliubov (DHB) model [9]. We have also used the results of previous systematics for charge distributions [10, 11], extracted from electron scattering experiments, as a check of our DHB results. Along the table of stable nuclides, the diffuseness for the nucleon and matter densities spread around the average values $\bar{a}_n = 0.50\ fm$ and $\bar{a}_m = 0.56\ fm$, respectively. A small dispersion of about $0.025\ fm$ around these average values is expected due to effects of the structure of the nuclei. We have determined the radii R_0 for the 2pF distributions assuming that the corresponding root-mean-square radii should be equal to those of the theoretical (DHB) densities. The nucleon and matter densities give very similar radii, which are well described by the following linear fit:

$$R_0 = 1.31\ A^{1/3} - 0.84\ fm. \quad (3)$$

Due to effects of the structure of the nuclei, the R_0 values spread around this linear fit with dispersion of $0.07\ fm$.

III The double-folding potential

The double-folding potential has the form [1]

$$V_F(R) = \int \rho_1(r_1)\ \rho_2(r_2)\ v_{NN}(\vec{R} - \vec{r_1} + \vec{r_2})\ d\vec{r_1}\ d\vec{r_2}\ , \quad (4)$$

where R is the distance between the centers of the nuclei, ρ_i are the respective nucleon distributions, and $v_{NN}(\vec{r})$ is the effective nucleon-nucleon interaction. The success of the folding model can only be judged meaningfully if the effective nucleon-nucleon interaction employed is truly realistic. The most widely used realistic interaction is known as M3Y [1, 2], which can usually assume two versions: Reid and Paris.

The six-dimensional integral (Eq. 4) can easily be solved by reducing it to a product of three one-dimensional Fourier transforms [1], but the results may only be obtained through numerical calculations. In order to provide analytical expressions for the folding potential, we consider, as an approximation, that the range of the effective nucleon-nucleon interaction is negligible in comparison with the diffuseness of the nuclear densities. In this zero-range approach, the double-folding potential can be obtained from:

$$v_{NN}(\vec{r}) \approx V_0\ \delta(\vec{r}) \Rightarrow V_F(R) = \frac{2\pi V_0}{R} \int_0^\infty r_1\ \rho_1(r_1) \left[\int_{|R-r_1|}^{R+r_1} r_2\ \rho_2(r_2)\ dr_2 \right] dr_1. \quad (5)$$

The Fermi distribution may be represented, with precision better than 3% for any r value, by:

$$\frac{\rho_0}{1 + exp\left(\frac{r-R_0}{a}\right)} \approx \rho_0\ C\left(\frac{r - R_0}{a}\right)\ , \quad (6)$$

$$C(x \leq 0) = 1 - \frac{7}{8}e^x + \frac{3}{8}e^{2x}\ , \quad (7)$$

$$C(x \geq 0) = e^{-x}\left(1 - \frac{7}{8}e^{-x} + \frac{3}{8}e^{-2x}\right). \quad (8)$$

This approximation is particularly useful in obtaining analytical expressions for integrals that involve the 2pF distribution. If both nuclei have the same diffuseness a, the double-integral (Eq. 5) can be solved analytically using the approximation represented by Eq. 6, and the result expressed as a sum of a large number of terms, most of them negligible for $a \ll R_0$. Rather simple expressions can be found after an elaborate algebraic manipulation:

$$V_F(R \leq R_2 - R_1 + a) \approx V_0\ \rho_{01}\ \rho_{02}\ \frac{4}{3}\pi R_1^3 \left\{ 1 + 9.7\left(\frac{a}{R_1}\right)^2 - \left[0.875\left(\frac{R_2^3}{R_1^3} - 1\right) + \frac{a}{R_1}\left(2.4 + \frac{R_2^2}{R_1^2}\right)\right] e^{-(R_2 - R_1)/a} \right\}\ , \quad (9)$$

$$V_F(R_2 - R_1 + a \leq R \leq R_1 + R_2) \approx V_0\ \rho_{01}\ \rho_{02}$$
$$\frac{4}{3}\pi\mathcal{R}^3\ \left(\frac{1}{1+\zeta\tau}\right)\left\{\tau^2\left[\frac{3}{8}+\frac{\tau}{4}+\zeta\frac{\tau^2}{16}\right]+2.4\,\eta^2\left[1-\frac{5}{8}\eta-\zeta\tau^2+\left(\frac{5}{4}\eta-\frac{1}{2}\right)e^{\varepsilon}+\left(1+\frac{5}{8}\eta\right)e^{-(\varepsilon+2R_1/a)}\right]\right\}\ , \quad (10)$$

$$V_F(R \geq R_1 + R_2) \approx V_0\ \rho_{01}\ \rho_{02}\ \pi a^2\ \mathcal{R}\ g(\tau)\ (1+s/a)\ e^{-s/a}\ , \quad (11)$$

where $s = R - (R_1 + R_2)$, $\mathcal{R} = 2R_1R_2/(R_1 + R_2)$, $\zeta = \mathcal{R}/(R_1 + R_2)$, $\tau = s/\mathcal{R}$, $\eta = a/\mathcal{R}$, $\varepsilon = s/a$, R_1 and R_2 are the radii of the nuclei (hereafter we consider $R_2 \geq R_1$). The function g is given by:

$$g(\tau) = \frac{1+\tau+\tau^2\zeta/3+\eta+(\eta+1/2)\ e^{-\varepsilon}}{1+\zeta\tau}\ . \quad (12)$$

We define the reduced folding potential at the surface region by:

$$V_{red}(s \geq 0) = \frac{V_F}{\rho_{01}\ \rho_{02}\ \pi a^2\mathcal{R}\ g(\tau)}\ . \quad (13)$$

Taking into account Eqs. 11 and 13, the reduced potential can be represented by the following system-independent expression:

$$V_{red}(s \geq 0) \approx V_0\ (1+s/a)\ e^{-s/a}\ . \quad (14)$$

However, it is not clear that one can find a simple form for such a system-independent quantity at inner distances from Eqs. 9 and 10. In Section V, the reduced potential is useful for addressing the potential strength systematization. Thus we define V_{red} for $s \leq 0$ through the following trivial form:

$$V_{red}(s \leq 0) = V_0\ . \quad (15)$$

The end of this section is devoted to the study of the effect on the folding potential of a finite range for the effective nucleon-nucleon interaction. The tri-dimensional delta function, $V_0\ \delta(\vec{r})$, can be represented through the limit $\sigma \to 0$ applied to the finite-range Yukawa function

$$Y_\sigma(r) = V_0\ \frac{e^{-r/\sigma}}{4\pi r\sigma^2}\ . \quad (16)$$

Fig. 1 shows a comparison of folding potentials in the zero-range approach (Eq. 5) with the result obtained (from Eq. 4) using an Yukawa function for the effective nucleon-nucleon interaction. The finite range is not truly significant at small distances, and can be accurately simulated at the surface, within the zero-range approach, just by slightly increasing the diffuseness of the nuclear densities.

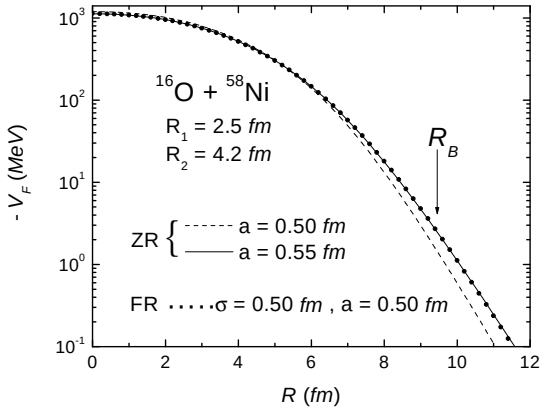

Figure 1. Double-folding potentials for 2pF distributions with different diffuseness values (a) that may represent the ^{16}O + ^{58}Ni system. The potentials have been calculated in the zero-range approach (ZR) or with a finite-range (FR) Yukawa function for the effective nucleon-nucleon interaction.

IV Nonlocal description of the nucleus-nucleus interaction

When dealing with nonlocal interactions, one is required to solve the following integro-differential equation

$$-\frac{\hbar^2}{2\mu}\nabla^2\Psi(\vec{R}) + [V_C(R) + V_{pol}(R,E) + \imath W_{pol}(R,E)]\,\Psi(\vec{R}) + \int U(\vec{R},\vec{R}')\ \Psi(\vec{R}')\ d\vec{R}' = E\Psi(\vec{R})\ . \quad (17)$$

V_C is the Coulomb interaction assumed to be local. V_{pol} and W_{pol} are the real and imaginary parts of the polarization potential and contain the contribution arising from nonelastic channel couplings. The corresponding nonlocality, called the Feshbach nonlocality, is implicit through the energy-dependence of these terms. $U(\vec{R},\vec{R}')$ is the bare interaction and the nonlocality here, the Pauli nonlocality, is solely due to the Pauli exclusion principle and involves the exchange of nucleons between target and projectile.

Guided by the microscopic treatment of the nucleon-nucleus scattering [12, 13, 14, 15, 16], the following ansatz is assumed for the heavy-ion bare interaction [6]

$$U(\vec{R},\vec{R}') = V_{NL}\left(\frac{\vec{R}+\vec{R}'}{2}\right)\frac{1}{\pi^{3/2}b^3}e^{-\left(|\vec{R}-\vec{R}'|/b\right)^2} , \quad (18)$$

where b is the range of the Pauli nonlocality. Introduced in this way, the nonlocality is a correction to the local model, and in the $b \to 0$ limit Eq. 17 reduces to the usual Schröedinger differential equation. The range of the nonlocality can be found through $b \approx b_0 m_0/\mu$ [17], where $b_0 = 0.85\ fm$ is the nucleon-nucleus nonlocality parameter [12], m_0 is the nucleon mass, and μ is the reduced mass of the nucleus-nucleus system.

The relation between the nonlocal interaction and the folding potential is obtained from [6]

$$V_{NL}(R) = V_F(R) . \quad (19)$$

Due to the central nature of the interaction, it is convenient to write down the usual expansion in partial waves, and the integro-differential equation can be recast into the following form [8]:

$$\frac{\hbar^2}{2\mu}\frac{d^2u_\ell(R)}{dR^2} + \left[E - V_C(R) - V_{pol}(R,E) - \imath W_{pol}(R,E) - \frac{\ell(\ell+1)\hbar^2}{2\mu R^2}\right]u_\ell(R) = \int_0^\infty V_\ell(R,R')\ u_\ell(R')\ dR' . \quad (20)$$

When confronting theory and experiment, one usually relies on the optical model with a local potential. This brings into light the issue of extracting from Eq. 20 a local-equivalent (LE) potential

$$V_{LE}(R,E) + \imath W_{LE}(R,E) = \frac{1}{u_\ell(R)}\int_0^\infty V_\ell(R,R')\ u_\ell(R')\ dR' . \quad (21)$$

The presence of the wave-function in Eq. 21 indicates that the LE potential is complex and also ℓ- and energy-dependent. For neutron-nucleus systems, the LE potential is only weakly ℓ-dependent, and an approximate relation to describe its energy-dependence has been obtained [12]. A generalization of this relation for the ion-ion case is given by [5, 6]:

$$V_{LE}(R,E) \approx V_F(R)\ e^{-\gamma[E-V_C(R)-V_{LE}(R,E)]} , \quad (22)$$

with $\gamma = \mu b^2/2\hbar^2$. The local-equivalent potential is quite well described by Eq. 22 for any ℓ value [8], except at very small distances ($R \approx 0$) that are not probed by heavy-ion experiments. At near-barrier energies, $E \approx V_C(R_B) + V_{LE}(R_B)$, the effect of the Pauli nonlocality is negligible and $V_{LE}(R,E) \approx V_F(R)$, but the higher the energy is, the greater is the effect. At energies about $200\ MeV/nucleon$ the local-equivalent potential is about one order of magnitude less intense than the corresponding folding potential (see examples in Refs. [5, 6]).

In a classical physics framework, the exponent in Eq. 22 is related to the kinetic energy (E_k) and to the local relative speed between the nuclei (v) by

$$v^2 = \frac{2}{\mu}E_k(R) = \frac{2}{\mu}\left[E - V_C(R) - V_{LE}(R,E)\right] ; \quad (23)$$

and Eq. 22 may be rewritten in the following form

$$V_{LE}(R,E) \approx V_F(R)\ e^{-[m_0 b_0 v/(2\hbar)]^2} \approx V_F(R)\ e^{-4v^2/c^2} , \quad (24)$$

where c is the speed of light. Therefore, in this context the effect of the Pauli nonlocality is equivalent to a velocity-dependent nuclear interaction (Eq. 24). Another possible interpretation is that the local-equivalent potential may be associated directly with the folding potential (Eq. 25), with an effective nucleon-nucleon interaction (Eq. 26) dependent on the relative speed (v) between the nucleons

$$V_{LE}(R,E) = V_F = \int \rho_1(r_1)\ \rho_2(r_2)\ v_{NN}(v, \vec{R} - \vec{r_1} + \vec{r_2})\ d\vec{r_1}\ d\vec{r_2} , \quad (25)$$

$$v_{NN}(v,\vec{r}) = v_f(\vec{r})\ e^{-4v^2/c^2} . \quad (26)$$

V Systematization of the nuclear potential

As already mentioned, the angular distribution for elastic scattering provides an unambiguous determination of the real part of the optical potential in a region around the sensitivity radius (R_S). For bombarding energies above (and near) the barrier, the sensitivity radius is rather energy-independent and close to the barrier radius (R_B), while at intermediate energies much inner distances are probed. At sub-barrier energies, the R_S is strongly energy-dependent, with its variation connected to the classical turning point;

this fact has allowed the determination of the potential in a wide range of near-barrier distances, $R_B \leq R_S \leq R_B + 2\ fm$. With the aim of avoiding ambiguities in the potential systematization, we have selected "experimental" (extracted from elastic scattering data analyses) potential strengths at the corresponding sensitivity radii, from works in which the R_S has been determined or at least estimated. In several articles, the authors claim that their data analyses at intermediate energies have unambiguously determined the nuclear potential in a quite extensive region of interaction distances. In such cases, we have considered potential strength "data" in steps of $1\ fm$ over the whole probed region.

The experimental potential strengths represent the real part of the optical potential, which corresponds to the addition of the bare and polarization potentials. The contribution of the polarization to the optical potential depends on the particular features of the reaction channels involved in the collision, and is therefore quite system-dependent. If this contribution were very significant, it would be too difficult for one to set a global description of the heavy-ion nuclear interaction. In the present work, we neglect the real part of the polarization potential and associate the experimental potential strengths (V_{Exp}) with the bare interaction (V_{LE}). The success of our findings seems to support such a hypothesis.

In analysing experimental potential results for such a wide energy range and large number of different systems, we consider quite appropriate the use of system- and energy-independent quantities. We have removed the energy-dependence from the experimental potential strengths through the calculation of the corresponding folding potential strengths, V_{F-Exp}, based on Eq. 22. The system-dependence of the potential data set has then been removed with the use of the experimental reduced potential, $V_{red-Exp}$. For $s \geq 0$ this quantity was calculated from Eq. 13, and for inner s values we have adopted the following simple definition

$$V_{red-Exp} = V_0 \ \frac{V_{F-Exp}}{V_{F-Teo}} \ , \qquad (27)$$

with V_{F-Teo} calculated through Eq. 5. The other useful quantity is the distance between surfaces: $s = R_S - (R_1 + R_2)$, where R_S is associated to the sensitivity radius, and the radii of the nuclei have been obtained from Eq. 4.

In Fig. 2 (bottom), the experimental reduced potential strengths are confronted with the theoretical prediction (Eqs. 14 and 15). The fit to the data in the inner region ($s \leq 0$) results unambiguously in the value $V_0 = -456\ MeV\ fm^3$, and is quite insensitive to the diffuseness parameter. The fit for $s \geq 0$ is sensitive to both: V_0 and a, and the corresponding best fit values are $a = 0.56\ fm$ and the same V_0 found for the inner region. The standard deviation of the data set around the best fit (solid line in Fig. 2 - bottom) is 25%, a value somewhat greater than the dispersion (20%) expected to arise from effects of the structure of the nuclei [8]. We believe that the remaining difference comes from two sources: uncertainties of the experimentally extracted potential strengths and the contribution of the polarization potential that we have neglected in our analysis. We point out that the best fit diffuseness value, $a = 0.56\ fm$, is equal to the average diffuseness found (Section II) for the matter distributions and greater than the average value ($a = 0.50\ fm$) of the nucleon distributions. This is a consistent result because we have calculated the reduced potential strengths based on the zero-range approach (through Eqs. 5, 13 and 27). As discussed in Section III, the effect of a finite-range for the effective nucleon-nucleon interaction can be simulated, within the zero-range approach, by increasing the diffuseness of the (nucleon) densities of the nuclei.

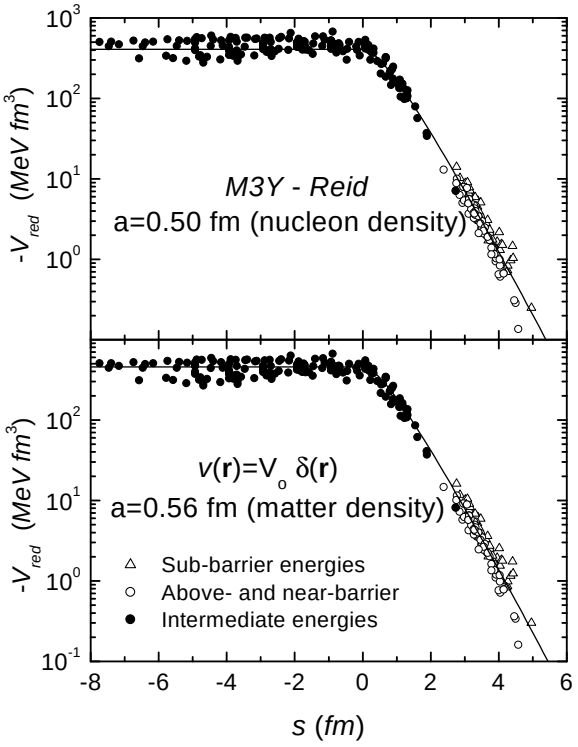

Figure 2. Comparison between experimental and theoretical reduced potentials in the context of the zero-range (bottom) or finite-range (top) approachs.

In order to characterize the importance of the Pauli nonlocality, we have also obtained the reduced potential strengths through calculations performed without the correction (Eq. 22) due to the energy-dependence of the LE potential, i.e. associating the experimental potential strengths directly with the folding potential. The quality of the corresponding fit is similar to that obtained with the nonlocality, but the V_0 and a parameters are significantly different. In the next Section, we show that the values found without considering the nonlocality, $a = 0.61\ fm$ and

$V_0 = -274\ MeV\ fm^3$, seem to result in an unrealistic nucleon-nucleon interaction.

VI The effective nucleon-nucleon interaction

After removing the energy-dependence of the experimental potential strengths, the corresponding results are compatible with the double-folding potential in the zero-range approach (Eq. 5), provided that the matter densities of the nuclei be adopted in the folding procedure instead of the nucleon densities. In this section, we study the consistency of our results for the nuclear potential in the case that the double-folding model is treated in the more common interpretation: the nucleon distributions and a finite-range nucleon-nucleon interaction are assumed in Eq. 4. With the purpose of keeping the comparison between experimental and theoretical results through the use of system-independent quantities, it is necessary to change the definition of the experimental reduced potential

$$V_{red-Exp} = V_{red-Teo}\ \frac{V_{F-Exp}}{V_{F-Teo}}\ , \qquad (28)$$

where V_{F-Teo} is now calculated through Eq. 4. $V_{red-Teo}$ is still obtained from Eqs. 14 and 15, with the V_0 parameter being associated to the volume integral of the effective nucleon-nucleon interaction (actually, this same procedure has also been adopted in the zero-range case)

$$V_0 = 4\pi \int v_{NN}(r)\ r^2\ dr\ . \qquad (29)$$

The effective nucleon-nucleon interaction should be based upon a realistic nucleon-nucleon force, since our goal is to obtain a unified description of the nucleon-nucleon, nucleon-nucleus and nucleus-nucleus scattering. A realistic interaction should match the empirical values for the volume integral and root-mean-square radius of the nucleon-nucleon interaction, $V_0 \approx -430\ MeV\ fm^3$ and $r_{rms} \approx 1.5\ fm$, that were extrapolated from the main features of the optical potential for the nucleon-nucleus scattering at $E_{nucleon} = 10\ MeV$ [1, 18, 19, 20]. The M3Y interaction has been derived [1] with basis on the *G*-matrix for two nucleons bound near the Fermi surface, and certainly is representative of realistic interactions. In table 1 are presented the volume integral and root-mean-square radius for several nucleon-nucleon interactions used in this work, including the M3Y at $10\ MeV/nucleon$.

Table 1: The width, volume integral and root-mean-square radius for several effective nucleon-nucleon interactions considered in this work.

Interaction	σ or a_m (fm)	V_0 (MeV fm^3)	r_{rms} (fm)
M3Y-Reid	-	- 408	1.62
M3Y-Paris	-	- 447	1.60
Yukawa	0.58	- 439	1.42
Gaussian	0.90	- 448	1.56
Exponential	0.43	- 443	1.49
Folding-type	0.30	- 456	1.47

The M3Y interaction is not truly appropriate for use in the context of the nonlocal model, because it already contains a simulation of the exchange effects included in its knock-on term. Furthermore, according to the nonlocal model the energy-dependence of the local-equivalent potential should be related only to the finite range of the Pauli nonlocality, but the knock-on exchange term in the M3Y interaction is also energy-dependent. Therefore, the use of the M3Y in the nonlocal model would imply a double counting of the energy-dependence that arises from exchange effects. In Section IV, we have demonstrated that the LE potential is identical with the double-folding potential for energies near the barrier, which are in a region around $10\ MeV/nucleon$. In this same energy range, the folding potential with the M3Y interaction have provided a very good description of elastic scattering data for several heavy-ion systems [1]. Thus, we believe that an appropriate nucleon-nucleon interaction for the nonlocal model could be the M3Y "frozen" at $10\ MeV/nucleon$ [6], i.e. considering the parameters of the Reid and Paris versions as energy-independent values. Fig. 2 (top) shows a comparison between experimental and theoretical heavy-ion reduced potentials, in which the "frozen" M3Y-Reid was considered for the nucleon-nucleon interaction. We emphasize that no adjustable parameter has been used in these calculations, but even so a good agreement between data and theoretical prediction has been obtained. The "frozen" M3Y-Paris provides similar results.

With the aim of investigating how much information about the effective nucleon-nucleon interaction can be extracted from our heavy-ion potential systematics, we have considered other possible functional forms for this effective interaction. Besides the Yukawa function (Eq. 16), we have

also used the Gaussian (Eq. 30) and the exponential (Eq. 31), which reduce to the tri-dimensional delta function in the limit $\sigma \to 0$,

$$G_\sigma(r) = V_0 \, \frac{e^{-r^2/2\sigma^2}}{(2\pi)^{3/2} \, \sigma^3} \, , \tag{30}$$

$$E_\sigma(r) = V_0 \, \frac{e^{-r/\sigma}}{8\pi\sigma^3} \, . \tag{31}$$

The fits to the heavy-ion potentials obtained with all these functions are of similar quality and comparable with that for the M3Y interaction. The resulting best fit widths (σ), volume integrals and corresponding root-mean-square radii are found in table 1. All the V_0 and r_{rms} values, including those of the M3Y, are quite similar. Also the "experimentally" extracted intensity of the nucleon-nucleon interaction in the region $1 \leq r \leq 3 \; fm$ seems to be rather independent of the model assumed for this interaction (see Fig. 3).

In Section V, we have demonstrated that the major part of the "finite-range" of the heavy-ion nuclear potential is related only to the spatial extent of the nuclei. In fact, even considering a zero-range for the interaction v_{NN} in Eq. 5, the shape of the heavy-ion potential could be well described just by folding the matter densities of the two nuclei. One would ask whether the finite-range shape of the effective nucleon-nucleon interaction can be derived in a similar way. Thus, we have considered a folding-type effective nucleon-nucleon interaction built from:

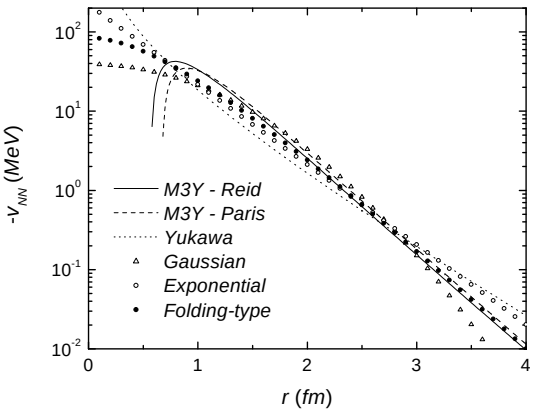

Figure 3. The complete set of effective nucleon-nucleon interactions considered in this work.

$$v_{NN}(\vec{r}) \approx v_f(r) = \int \rho_m(r_1) \; \rho_m(r_2) \; V_0 \; \delta(\vec{R} - \vec{r_1} + \vec{r_2}) \; d\vec{r_1} \; d\vec{r_2} = \frac{2\pi V_0}{r} \int_0^\infty r_1 \; \rho_m(r_1) \left[\int_{|r-r_1|}^{r+r_1} r_2 \; \rho_m(r_2) \; dr_2 \right] dr_1 \, , \tag{32}$$

where $V_0 = -456 \; MeV \; fm^3$ as determined by the heavy-ion potential analysis, and ρ_m is the matter density of the nucleon. Based on the intrinsic charge distribution of the proton in free space, which has been determined by electron scattering experiments, we have assumed an exponential shape for the matter density of the nucleon

$$\rho_m(r) = \rho_0 \; e^{-r/a_m} \, . \tag{33}$$

Of course, ρ_0 and a_m are connected by the normalization condition of the density. The integration of Eq. 32 results in

$$v_f(r) = \frac{V_0}{64 \; \pi \; a_m^3} \; e^{-r/a_m} \; \left(1 + \frac{r}{a_m} + \frac{r^2}{3a_m^2} \right) \, . \tag{34}$$

The folding-type and the M3Y interactions provide very similar fits of the reduced heavy-ion potential strengths. The folding-type nucleon-nucleon interaction results in realistic volume integral and root-mean-square radius (see table 1), and it is also quite similar to both versions of the M3Y interaction in the surface region (see Fig. 3).

The folding-type interaction in the context of the nonlocal model provides a very interesting unification between the descriptions of the nucleus-nucleus, nucleon-nucleus and effective nucleon-nucleon interactions. This can be appreciated through the comparison between Eqs. 24 and 26, with the subtle detail that V_F (in Eq. 24) and v_f (in Eq. 26) can both be calculated by folding the matter densities in the zero-range approach, and with the same V_0 value. Therefore, the interaction between two nuclei (or nucleons) can be obtained from

$$V_{LE}(R) = \int \rho_1(r_1) \; \rho_2(r_2) \; V_0 \; \delta(\vec{R} - \vec{r_1} + \vec{r_2}) \; e^{-4v^2/c^2} \; d\vec{r_1} \; d\vec{r_2} \tag{35}$$

where $V_0 = -456 \; MeV \; fm^3$, ρ_i are the matter densities, and v is the relative speed between the nuclei (or nucleons). All these findings seems to be quite consistent. However, the best fit value obtained for the diffuseness ($a_m = 0.30 \; fm$) of the matter density of the nucleon inside the nucleus is considerable greater than that ($a_{chp} = 0.235 \; fm$) found for the charge distribution of the proton in free space. This finding is consistent with the swelling of the nucleon observed

in the EMC effect [21], but should be contrasted with the opposite picture of a smaller nucleon inside the nucleus as advanced within the concept of color transparency [22].

VII Conclusion

The experimental potential strengths considered in the present systematics have been obtained at the corresponding sensitivity radii, a region where the nuclear potential is determined from the data analyses with the smallest degree of ambiguity. The Fermi distribution was assumed to represent the nuclear densities, with parameters consistent with an extensive amount of theoretical (DHB calculations) and experimental (electron scattering experiments) results. The potential data set is well described in the context of the nonlocal model, by the double-folding potential in the zero-range as well as in the finite-range approaches. The dispersion of the potential data around the theoretical prediction is 25%, which is compatible with the expected effects arising from the variation of the densities due to the structure of the nuclei. If the nonlocal interaction is assumed, the heavy-ion potential data set seems to determine a few characteristics of the effective nucleon-nucleon interaction, such as volume integral and root-mean-square radius, in a model-independent way.

The description of the bare potential presented in this work is based only on two fundamental ideas: the folding model and the Pauli nonlocality. We have avoided as much as possible the use of adjustable parameters, and in the case of the "frozen" M3Y interaction no adjustable parameters were necessary to fit the experimental potential strengths. Nowadays, the other important part of the heavy-ion interaction, the polarization potential, is commonly treated within a phenomenological approach, with several adjustable parameters which usually are energy-dependent and vary significantly from system to system. The association of the nonlocal bare potential presented in this work with a more fundamental treatment of the polarization should be the next step toward a global description of the nucleus-nucleus interaction.

This work was partially supported by Fundação de Amparo à Pesquisa do Estado de São Paulo (FAPESP).

References

[1] G. R. Satchler and W. G. Love, Phys. Rep. **55**, 183 (1979).

[2] M. E. Brandan and G. R. Satchler, Phys. Rep. **285**, 143 (1997) , and references therein.

[3] P. R. Christensen and A. Winther, Phys. Lett. B**65**, 19 (1976).

[4] C. P. Silva, M. A. G. Alvarez, L. C. Chamon, D. Pereira, M. N. Rao, E. S. Rossi Jr., L. R. Gasques, M. A. E. Santo, R. M. Anjos, J. Lubian, P. R. S. Gomes, C. Muri, B. V. Carlson, S. Kailas, A. Chatterjee, P. Singh, A. Shivastava, K. Mahata and S. Santra, Nucl. Phys. A**679**, 287 (2001).

[5] M. A. C. Ribeiro, L. C. Chamon, D. Pereira, M. S. Hussein and D. Galetti, Phys. Rev. Lett. **78**, 3270 (1997).

[6] L. C. Chamon, D. Pereira, M. S. Hussein M. A. C. Ribeiro and D. Galetti, Phys. Rev. Lett. **79**, 5218 (1997).

[7] L. C. Chamon, D. Pereira and M. S. Hussein, Phys. Rev. C**58**, 576 (1998).

[8] L. C. Chamon, B. V. Carlson, L. R. Gasques, D. Pereira, C. De Conti, M. A. G. Alvarez, M. S. Hussein, M. A. Candido Ribeiro, E. S. Rossi Jr., C. P. Silva, Phys. Rev. C**66**, 014610 (2002).

[9] B. V. Carlson and D. Hirata, Phys. Rev. C**62**, 054310 (2000).

[10] H. De Vries, C. W. De Jager and C. De Vries, Atomic Data and Nucl. Data Tables **36**, 495 (1987).

[11] E. G. Nadjakov, K. P. Marinova and Y. P. Gangrsky, Atomic Data and Nucl. Data Tables **56**, 133 (1994).

[12] F. Perey and B. Buck, Nucl. Phys. **32**, 253 (1962).

[13] T. H. R. Skyrme, Philos. Mag. **1**, 1043 (1956).

[14] G. Ripka, Nucl. Phys. **42**, 75 (1963).

[15] W. Bauhoff, H. V. von Geramb and G. Palla, Phys. Rev. C**27**, 2466 (1983).

[16] W. E. Frahn and R. H. Lemmer, Nuovo Cimento **5**, 1564 (1957).

[17] D. F, Jackson and R. C. Johnson, Phys. Lett. B**49**, 249 (1974).

[18] F. D. Bechetti and G. W. Greenlees, Phys. Rev. **182**, 1190 (1969).

[19] G. W. Greenlees, G. J. Pyle and Y. C. Yang, Phys. Rev. **171**, 1115 (1968).

[20] G. W. Greenlees, W. Makofske and G. J. Pyle, Phys. Rev C**1**, 1145 (1970).

[21] J. J. Aubert, G. Bassompierre, K. H. Becks, C. Best, E. Böhm, X. de Bouard, F. W. Brasse, C. Broll, S. Brown, J. Carr, R. W. Clifft, J. H. Cobb, G. Coignet, F. Combley, G. R. Court, G. D'Agostini, W. D. Dau, J. K. Davies, Y. Déclais, R. W. Dobinson, U. Dosselli, J. Drees, A. W. Edwards, M. Edwards, J. Favier, M. I. Ferrero, W. Flauger, E. Gabathuler, R. Gamet, J. Gayler, V. Gerhardt, C. Gössling, J. Haas, K. Hamacher, P. Hayman, M. Henckes, V. Korbel, U. Landgraf, M. Leenen, M. Maire, H. Minssieux, W. Mohr, H. E. Montgomery, K. Moser, R. P. Mount, P. R. Norton, J. McNicholas, A. M. Osborne, P. Payre, C. Peroni, H. Pessard, U. Pietrzyk, M. Rith, M. Schneegans, T. Sloan, H. E. Stier, W. Stockhausen, J. M. Thénard, J. C. Thampson, L. Urban, M. Villers, H. Wahlen, M. Whalley, D. Williams, W. S. C. Williams, J. Williamson, and S. J. Wimpenny, Phys. Lett. B**123**, 275 (1983).

[22] See, e.g., L. L. Frankfurt and M. I. Strikman, Phys. Rep. **76**, 214 (1981); **160**, 235 (1988).